ACS APPLIED MATERIALS & INTERFACES

www.acsami.org Research Article

Synthesis, Postsynthetic Modifications, and Applications of the First Quinoxaline-Based Covalent Organic Framework

Valerie A. Kuehl, Phuoc H. H. Duong, Deana Sadrieva, Samrat A. Amin, Yuqi She, Katie D. Li-Oakey, Jeffery L. Yarger, Bruce A. Parkinson, and John O. Hoberg*

Cite This: ACS Appl. Mater. Interfaces 2021, 13, 37494–37499 Read Online

ACCESS | Metrics & More | Article Recommendations | Supporting Information

ABSTRACT: We report a new synthetic protocol for preparing highly ordered two-dimensional nanoporous covalent organic frameworks (2D-COFs) based on a quinoxaline backbone. The quinoxaline framework represents a new type of COF that enables postsynthetic modification by placing two different chemical functionalities within the nanopores including layer-to-layer cross-linking. We also demonstrate that membranes fabricated using this new 2D-COF perform highly selective separations resulting in dramatic performance enhancement post cross-linking.

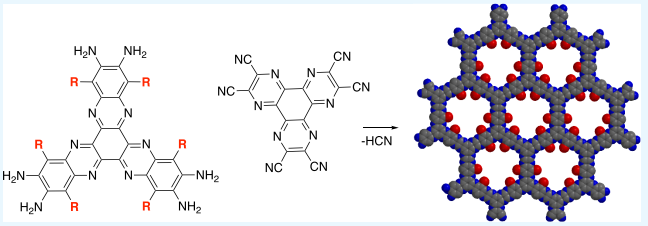

KEYWORDS: *quinoxaline, nanoporous, modifiable materials, membrane filtration, covalent organic framework, COF*

INTRODUCTION

Covalent organic frameworks (COFs) are two-dimensional honeycomb polymers that ideally assemble to produce highly ordered porous materials.[1] Research related to COFs has recently undergone rapid growth with the emergence of many new motifs that further expand the applications of COFs.[2−5] Predominate among these is the Schiff base reaction (condensation of amines with aldehydes or ketones) but more recently reactions such as the Knoevenagel condensation[6−8] or multicomponent reactions leading to thiazole-,[9] imidazole-,[10] and quinoline-linked[11] COFs have been reported. Additionally, postsynthetic COF modifications (PSM) have been developed that enable adding a variety of organic functional groups,[12] enabling the modification of COF properties and tuning them for various applications. As this development continues, there is still a need for new COF frameworks, via alternative synthetic routes and starting monomers, which will result in new properties.

RESULTS AND DISCUSSION

Quinoxalines have a long history in their synthesis and biological activity[13] and have found applications in fields such as organic field-effect transistors,[14] organic photovoltaics,[15] light-emitting diodes,[16] and dyes.[17] A less-used method for their synthesis involves nucleophilic aromatic substitution (S_NAr) of dinitriles with 1,2-phenylenediamines to produce dihydroquinoxalino[2,3-*b*]quinoxalines, known as fluoflavines, Scheme 1[18] We recognized that this reaction could be useful for COF formation via a S_NAr COF-forming reaction[19−21] and also provide reactive NH moieties for PSM.

The synthesis of hexaazatriphenylene-hexacarbonitrile (**HAT-CN**) was first reported by Kanakarajan and Czarnik,[22]

Scheme 1. Model Compound Studies

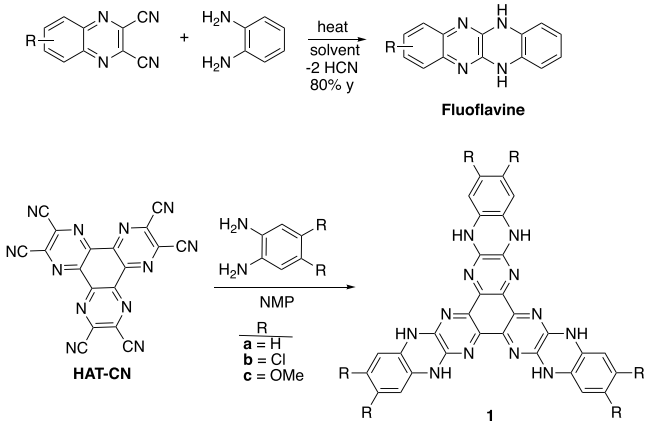

which is a C_3-symmetric hexanitrile precursor ideal for S_NAr reactions with either C_3-hexaamines or C_2-tetraamines. Furthermore, **HAT-CN** is prepared in one step that is scalable to a kilogram scale. Interestingly, **HAT-CN** has been used in the synthesis of nanoporous carbon nitrides by high-temperature pyrolysis between 550 and 1000 °C.[23] To test the feasibility of **HAT-CN** to undergo a tri-S_NAr reaction, it was reacted with a range of electron-donating and electron-

Received: May 12, 2021
Accepted: July 19, 2021
Published: July 28, 2021

https://doi.org/10.1021/acsami.1c08854
ACS Appl. Mater. Interfaces 2021, 13, 37494–37499

Scheme 2. COF-Forming Reactions

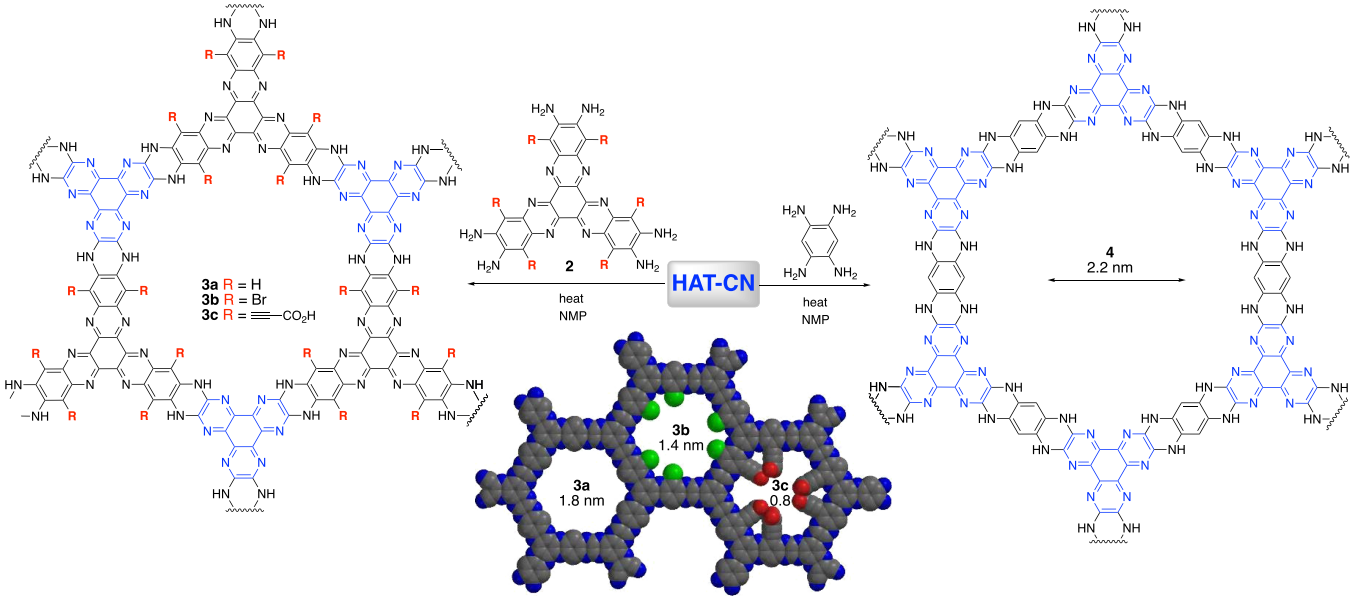

withdrawing disubstituted 1,2-phenylenediamines to produce **1a–c**, thus confirming its suitability in COF-forming reactions.

We have previously reported the use of hexamine **2** as a method to introduce functionality into the pores of COFs;[3,4] thus, **HAT-CN** was reacted with **2** under thermal conditions to produce COFs **3a–c** with functionality ranging from R = H, Br, and propargylic acid, as shown in Scheme 2. Additionally, the larger pore COF **4** was constructed with the use of 1,2,4,5-tetraaminobenzene. An inert gas was used to purge the headspace of the vessel, expelling HCN gas that was trapped in a separate solution of ferrous sulfate (see Supporting Information Figure S1 for setup). A reaction of HCN with $Fe(SO_4)$ produces a visibly noticeable blue-colored Prussian blue pigment and appearance of its nitrile stretch at ~2075 cm^{-1} in the Fourier transform infrared (FTIR) spectra. Further confirmation via FTIR spectroscopy shows the absence of the nitrile stretch in the resulting COFs, which appears at 2035 cm^{-1} in **HAT-CN** (see Supporting Information Figures S1,2 for IR comparisons). Characteristic COF bands at 1610, 1430, and 1353 cm^{-1} also indicated the formation along with the presence of a broad N–H stretch between 3000 and 3500 cm^{-1}.

Given the irreversibility of an S_NAr COF-forming reaction, as first reported by Yaghi and co-workers in their dioxin-linked COFs,[19] the probability of disordered materials was expected. We therefore performed extensive studies on solvent, stirring, time, and temperature (Supporting Information experimental section and Figures S3–8), concluding that 200 °C in *N*-methyl pyrrolidinone (NMP) with stirring for 24 h was near optimal. Thermogravimetric analysis coupled with differential scanning calorimetry was performed under air and argon for COFs **3a–3c** (Supporting Information Figures S9–11) to determine thermal stability. Measurements under atmospheric conditions revealed decomposition at 455, 500, and 533 °C for **3a, 3b,** and **3c**, respectively.

Bright-field transmission electron microscopy (BFTEM) (Figure 1A and Supporting Information Figures S12–14) revealed large plate-like features for COFs **3a–3c**. **3a** and **3b** (Figure 1B) and also displayed hexagonal diffraction patterns with two orders of periodicity, while COF **3c** exhibited a tetragonal diffraction pattern, perhaps due to sodium ions from the NaOH solutionused to disperse the COF to prepare the

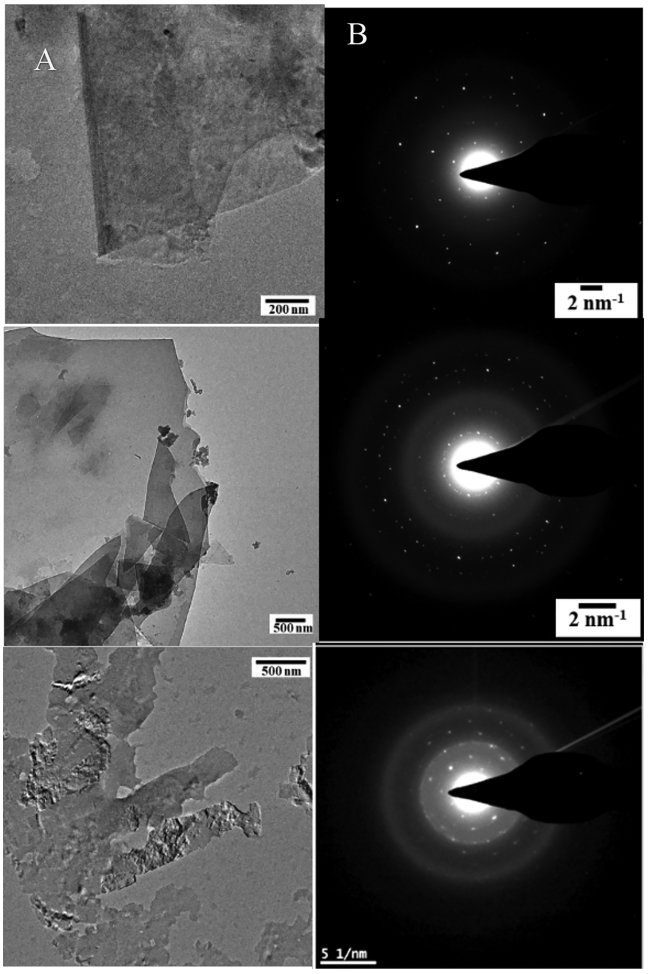

Figure 1. (A):(left side) BFTEM images with electron diffraction patterns of **3a** (top), **3b** (middle), and **3c** (bottom). (B): (right side): diffraction patterns of **3a** (top), **3b** (middle), and **3c** (bottom).

https://doi.org/10.1021/acsami.1c08854
ACS Appl. Mater. Interfaces 2021, 13, 37494–37499

TEM grids interacting with the carboxylic functional groups. The inner-most diffraction pattern of COF **3b** showed the largest spacing measured at 0.6 nm. COFs **3a**−**3c** all exhibited spacings measured of 0.3 nm.

Figure 2A illustrates the powder X-ray diffraction (PXRD) of COFs **3b** and **3c** with rather broad peaks confirming a degree of disorder that is typical for COFs. Low-angle broad peaks centered at around 5.9° for 2 theta indicate a spacing of 0.75 nm. Figure 2B and C show the nitrogen sorption isotherm illustrating the pore size distribution profile for **3c**. Barrett−Joyner−Halenda (BJH) analysis of COF **3c** (Figure 2C) is consistent with a pore size of ∼0.8 nm, consistent with DFT calculations as illustrated in the COF model shown in Scheme 1. COF **3b** sorption data were also consistent with its calculated pore size (Supporting Information Figure S15). Solid-state $^{1}H \rightarrow {}^{13}C$ cross-polarization magic-angle spinning (CP-MAS) nuclear magnetic resonance (NMR) spectroscopy on the solid materials was performed on **3a** to further confirm the expected structures, (see also Supporting Information Figures S16,17 for **3b**). The observed resonances at 168, 154, and 140−125 ppm can be assigned to the COF framework. However, along with the signals corresponding to the aromatic carbons, resonances between 15 and 50 and 175 ppm were unexpectedly observed, which correspond to the NMP solvent. All COF materials were subjected to postsynthesis Soxhlet extraction with water and then EtOH followed by oven drying, *sc*CO_2 extraction, and then further oven drying. Even with these extensive procedures, all residual solvent molecules were not removed and were likely encapsulated between the layers.

We next investigated PSM involving the secondary amine moieties. Reaction of **3a** with trifluoroacetic anhydride yielded the trifluoroacetamide COF **5**, as shown in Figure 3. Characterization of **5** with XPS was definitive for fluorine and carbonyl oxygen incorporation with both C−F and C−O peaks observed (see Supporting Information Figures S18−23). FTIR results were also conclusive as strong C−F stretches were observed at 1184 and 1133 cm^{-1} along with expected stretches at 1667 and 1571 cm^{-1} and the disappearance of the N−H stretch, Figure 4.

Although the 2D structure of most COFs and inherent 2D stacking makes them ideal for membrane formation, it is still problematic that the stacked flakes could be redispersed or the membranes could swell in some chemical environments. Therefore, a PSM with oxalyl chloride was performed with the goal of cross-linking the 2D sheets via a reaction with the N−H bonds within the pore. Oxalyl is too small to span across the pore to produce oxalamide moieties within a pore; however, there are three other possibilities for its incorporation.

First, cross-linking of flakes as shown in Figure 3**A** produces covalently bound parallel flakes; however, the formation of COF polymers linked edge-to-edge in the same plane as shown in Figure 3**B** is also feasible and itself could improve membrane performance. Capping of the 1,2-diamines on the edges of a single sheet (Figure 3**C**) also likely occurs in both cases. Given the average flake sizes from TEM images, the flake cross-linking reaction should be prevalent. FTIR results were conclusive for amide formation with the appearance of a 1700 cm^{-1} stretch and the noticeable disappearance of the NH moiety (Supporting Information Figure S24). The ^{13}C CP-MAS NMR spectrum of **3bXL** (Supporting Information Figure S17) further indicated the inclusion of Et_3N, lending additional credibility to the encapsulation of the solvent between layers.

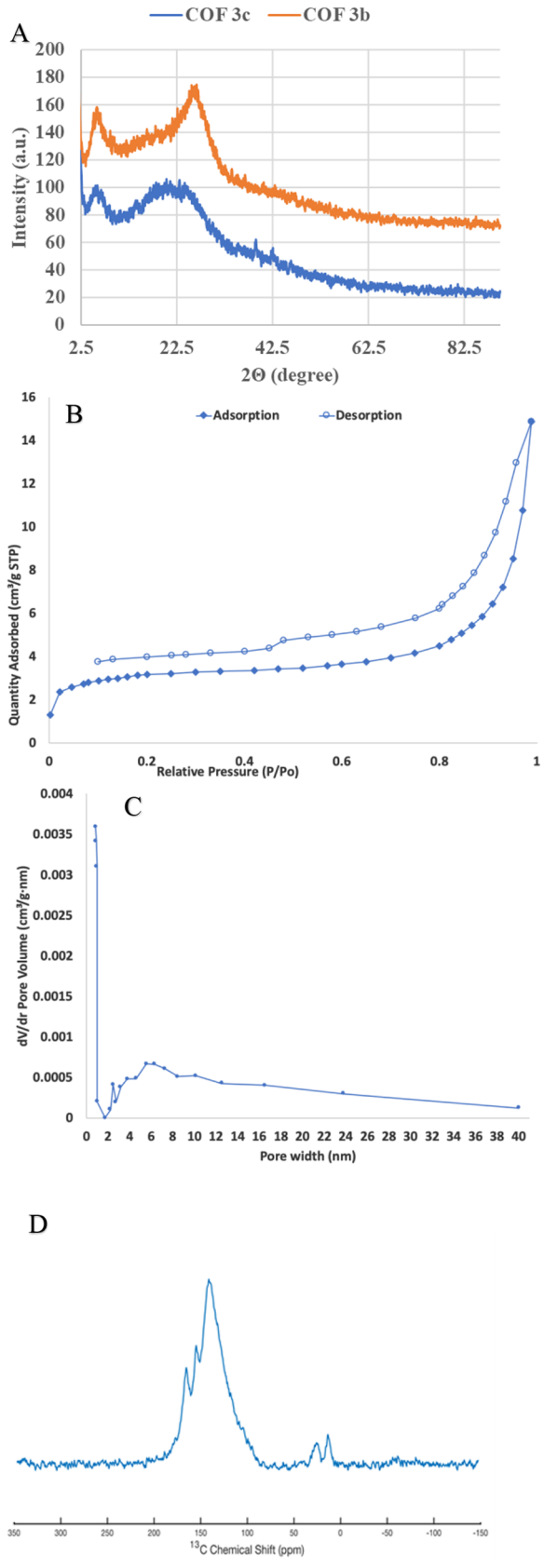

Figure 2. (A): **3b** and **3c** experimental PXRD spectra, (B): **3c** N_2 sorption isotherm curves, (C): **3c** pore size distribution, and (D): **3a** $^{1}H \rightarrow {}^{13}C$ CP-MAS NMR spectrum.

https://doi.org/10.1021/acsami.1c08854
ACS Appl. Mater. Interfaces 2021, 13, 37494−37499

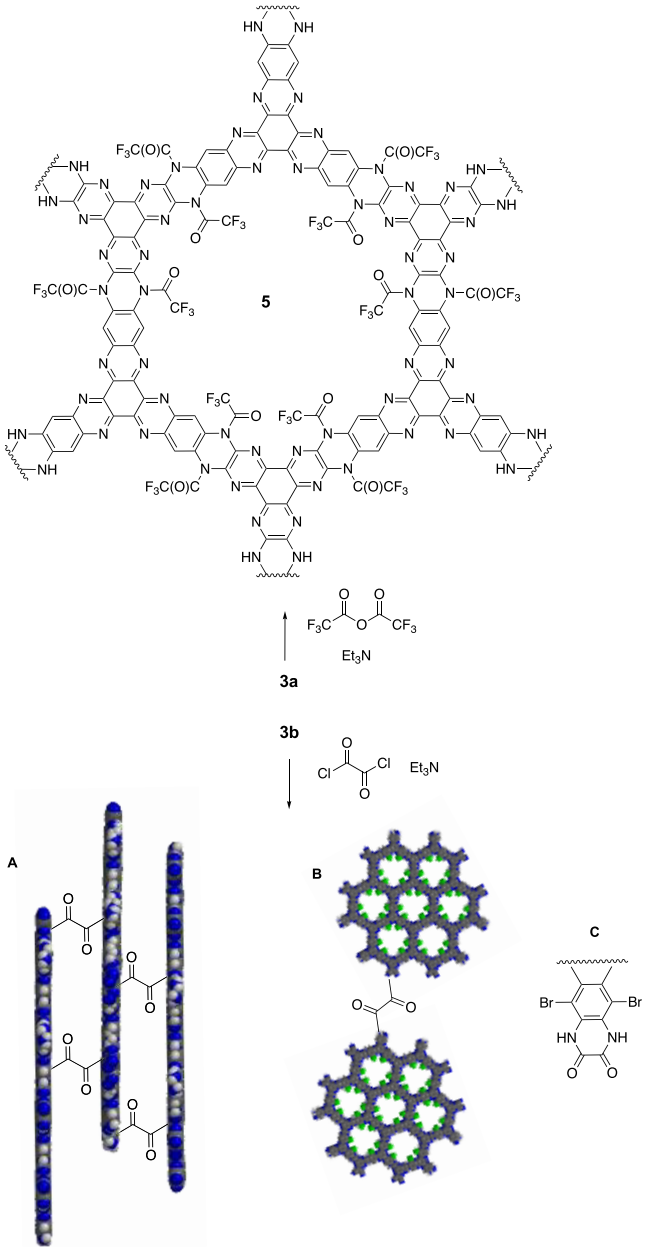

Figure 3. Synthesis of COF **5** and illustrations of cross-linked **3bXL** (A), linear polymers (B), and capped diamines (C).

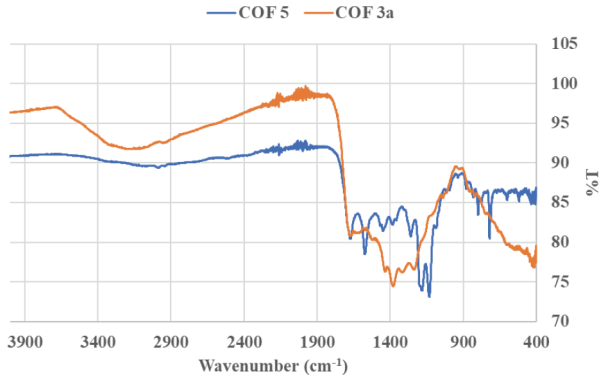

Figure 4. FTIR spectra of **3a** and **5**.

Most notable was the BFTEM (Supporting Information Figure S25) result that revealed noticeably thicker flakes throughout, providing more evidence for type **A** cross-linking between layers.

Construction and evaluation of membranes constructed from **3b** and **3bXL** provide functional experimental insights into the COF structure and PSM chemistry. The COFs **3b** and **3bXL** were supported on porous anodic aluminum oxide (20 nm pore size) via vacuum filtration. The solvent flux and separation capabilities of these membranes were then compared. Water permeance measured for **3b** and **3bXL** was 1470 ± 430 and 580 ± 220 L m^{-2} h^{-1} bar^{-1}, respectively. Rejection capabilities were measured using a series of dyes and an initial screening is listed in Table 1, with entries 2 and 4

Table 1. Comparison of the Selectivity Given in Percent Rejection between 3b and 3bXL Membranes Using Organic Dyes in L m^{-2} h^{-1} bar^{-1}

entry	dye with MW (g/mol)	3b	3bXL
1	Orange II; 350	2.3	36.3
2	Congo red; 697	22.1 ± 8.1	98.3 ± 1.8
3	Safranin O; 351	6.6	58.9
4	Alcian Blue; 1299	29.9 ± 7.1	97.5 ± 2.7

subjected to statistical significance. Entries 1 and 2 represent negatively charged dyes, while entries 3 and 4 are positively charged dyes. As shown, cross-linking of **3b** (aka **3bXL**) produces dramatic changes in the rejection performance for both types of dyes with nearly 100% rejection in entries 2 and 4 in the cross-linked membranes. This selectivity increase and permeance decrease in the cross-linked membranes are likely due to both **A** and **B** shown in Figure 3, which prevent the interstitial flow of both water and dye, forcing both the permeate and retentate through the pores of the COF rather than an interlayer path. The top illustration in Figure 5 shows a space filling model of a single pore of COF **3b** flanked by four dyes. It is apparent that Orange II and Safranin O are small enough to fit through the pore, whereas Congo Red and Alcian Blue are both too large, in agreement with our results. We have previously observed these types of rejection levels with carboxylic acid-lined pores and the impact of flow through pores versus between flakes.[3,4] Photographs of dye separation with COF **3bXL** using feed solutions containing Congo Red and Alcian Blue are also shown in Figure 5, illustrating the potential of these cross-linked COF-based membranes for nanofiltration applications.

However, it should be noted that recently Dichtel and co-workers reported on certain COFs functioning as dye adsorbents and not size-selective molecular sieves.[24] With this possibility in mind, scanning electron microscopy (SEM) images of the membranes fabricated using **3b** and **3bXL** were obtained (Figure 6). As seen in the cross-sectional images, **3b** show a membrane with a thickness of about 4.7 microns whereas the **3bXL** membrane had a thickness of about 1 micron, and it would be expected that the thicker membrane would be a better adsorbent than the thinner **3bXL** if adsorption was occuring. Furthermore, permeance of the thinner membrane (**3bXL**) was reduced, contrary to what would be expected with no cross-linking. Finally, no visual dye staining of the membranes was observed after dye filtration. Thus, it would appear that the effect of cross-linking as shown in Figure 3 is promoting better size-selective molecular sieving.

https://doi.org/10.1021/acsami.1c08854
ACS Appl. Mater. Interfaces 2021, 13, 37494−37499

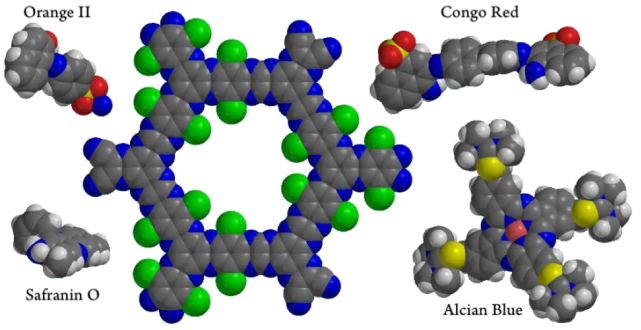

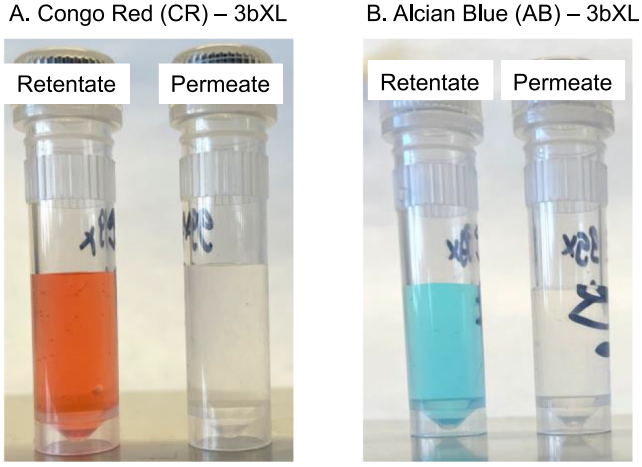

Figure 5. Structures of the dyes surrounding a single pore of COF **3b** (top). Digital photographs of dye separation with COF **3bXL** using feed solutions containing: (A) negatively charged dye Congo Red and (B) positively charged dye Alcian Blue.

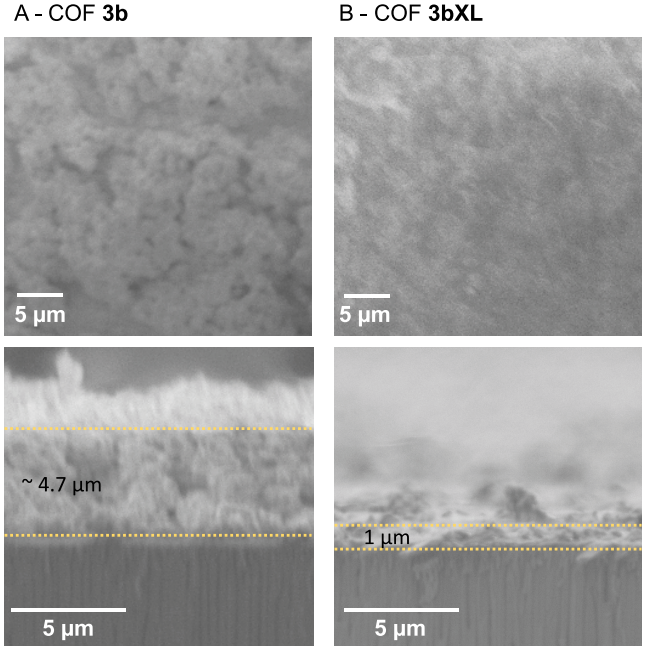

Figure 6. Surface (top) and cross-sectional (bottom) SEM images of (A) COF **3b** and (B) **3bXL** membranes.

CONCLUSIONS

We have designed and synthesized new COF structures using S_NAr reactions to produce a quinoxaline backbone in the framework. These newly designed and highly stable COFs incorporate one type of functionality with the use of hexamine **2** and also produces NH moieties within the pores. These NH moieties undergo PSM both within the pore structure or cross-linking between flakes resulting in dramatic performance enhancements in membranes fabricated from the COFs. Further reports on these dual-functional COFs along with the remarkable hydrophobicity of COF **5** will be forthcoming.

ASSOCIATED CONTENT

Supporting Information

The Supporting Information is available free of charge at https://pubs.acs.org/doi/10.1021/acsami.1c08854.

Experimental section including model compound studies and COF formation, plots of NMR, IR, TEM, EDS/EDX, BET analysis, and membrane fabrication and testing (PDF)

AUTHOR INFORMATION

Corresponding Author

John O. Hoberg − *Department of Chemistry, University of Wyoming, Laramie, Wyoming 82071, United States;* orcid.org/0000-0003-3833-8122; Email: hoberg@uwyo.edu

Authors

Valerie A. Kuehl − *Department of Chemistry, University of Wyoming, Laramie, Wyoming 82071, United States*

Phuoc H. H. Duong − *Department of Chemical Engineering, University of Wyoming, Laramie, Wyoming 82071, United States;* orcid.org/0000-0002-0949-3505

Deana Sadrieva − *Department of Chemistry, University of Wyoming, Laramie, Wyoming 82071, United States*

Samrat A. Amin − *Magnetic Resonance Research Center, Arizona State University, Tempe, Arizona 85287, United States*

Yuqi She − *Department of Chemistry, University of Wyoming, Laramie, Wyoming 82071, United States*

Katie D. Li-Oakey − *Department of Chemical Engineering, University of Wyoming, Laramie, Wyoming 82071, United States;* orcid.org/0000-0002-0529-9203

Jeffery L. Yarger − *Magnetic Resonance Research Center and School of Molecular Sciences, Arizona State University, Tempe, Arizona 85287, United States;* orcid.org/0000-0002-7385-5400

Bruce A. Parkinson − *Department of Chemistry and School of Energy Resources, University of Wyoming, Laramie, Wyoming 82071, United States;* orcid.org/0000-0002-8950-1922

Complete contact information is available at: https://pubs.acs.org/10.1021/acsami.1c08854

Author Contributions

The manuscript was written through contributions of all authors. All authors have given approval to the final version of the manuscript.

Notes

The authors declare no competing financial interest.

ACKNOWLEDGMENTS

The authors acknowledge generous support from the Department of Energy-BES grant #DE-SC0020100, a fellowship from the National Institute of General Medical Sciences

(P20GM103432) from the National Institutes of Health for V.A.K., and support for D.S. from the Wyoming NASA Space Grant Consortium, NASA Grants #80NSSC20M0113 and #80NSSC19M0061. PXRD and BJH analyses were performed in the Nebraska Nanoscale Facility: National Nanotechnology Coordinated Infrastructure and the Nebraska Center for Materials and Nanoscience (and/or NERCF), which are supported by the National Science Foundation under Award ECCS: 2025298, and the Nebraska Research Initiative and support from the Magnetic Resonance Research Center, part of the Chemical and Environmental Characterization Core Facilities at Arizona State University, are acknowledged. J.L.Y. acknowledges support from the National Science Foundation (NSF-DMR-BMAT-1809645) and the Department of Defense-Army Research Office (DOD-ARO) grant No. W911-NF19-10152.

REFERENCES

(1) Côté, A. P.; Benin, A. I.; Ockwig, N. W.; O'Keeffe, M.; Matzger, A. J.; Yaghi, O. M. Porous, Crystalline, Covalent Organic Frameworks. *Science* **2005**, *310*, 1166−1170.

(2) Lohse, M. S.; Bein, T. Covalent Organic Frameworks: Structures, Synthesis, and Applications. *Adv. Funct. Mater.* **2018**, *28*, No. 1705553.

(3) Kuehl, V. A.; Yin, J.; Duong, P. H. H.; Mastorovich, B.; Newell, B.; Li-Oakey, K. D.; Parkinson, B. A.; Hoberg, J. O. A Highly Ordered Nanoporous, Two-Dimensional Covalent Organic Framework with Modifiable Pores, and Its Application in Water Purification and Ion Sieving. *J. Am. Chem. Soc.* **2018**, *140*, 18200−18207.

(4) Duong, P. H. H.; Kuehl, V. A.; Mastorovich, B.; Hoberg, J. O.; Parkinson, B. A.; Li-Oakey, K. D. Carboxyl-Functionalized Covalent Organic Framework as a Two-Dimensional Nanofiller for Mixed-Matrix Ultrafiltration Membranes. *J. Membr. Sci.* **2019**, *574*, 338−348.

(5) Brophy, J.; Summerfield, K.; Yin, J.; Kephart, J.; Stecher, J.; Adams, J.; Yanase, T.; Brant, J.; Li-Oakey, K.; Hoberg, J.; Parkinson, B. The Influence of Disorder in the Synthesis, Characterization and Applications of a Modifiable Two-Dimensional Covalent Organic Framework. *Dent. Mater.* **2021**, *14*, 71.

(6) Jin, E.; Asada, M.; Xu, Q.; Dalapati, S.; Addicoat, M. A.; Brady, M. A.; Xu, H.; Nakamura, T.; Heine, T.; Chen, Q.; Jiang, D. Two-Dimensional Sp^2 Carbon−Conjugated Covalent Organic Frameworks. *Science* **2017**, *357*, 673−676.

(7) Jin, E.; Li, J.; Geng, K.; Jiang, Q.; Xu, H.; Xu, Q.; Jiang, D. Designed Synthesis of Stable Light-Emitting Two-Dimensional Sp2 Carbon-Conjugated Covalent Organic Frameworks. *Nat. Commun.* **2018**, *9*, 4143.

(8) Cui, W.-R.; Zhang, C.-R.; Jiang, W.; Li, F.-F.; Liang, R.-P.; Liu, J.; Qiu, J.-D. Regenerable and Stable Sp2 Carbon-Conjugated Covalent Organic Frameworks for Selective Detection and Extraction of Uranium. *Nat. Commun.* **2020**, *11*, 436.

(9) Wang, K.; Jia, Z.; Bai, Y.; Wang, X.; Hodgkiss, S.; Chen, L.; Chong, S. Y.; Wang, X.; Yang, H.; Xu, Y.; Feng, F.; Ward, J. W.; Cooper, A. I. Synthesis of Stable Thiazole-Linked Covalent Organic Frameworks via a Multicomponent Reaction. *J. Am. Chem. Soc.* **2020**, *142*, 11131.

(10) Wang, P.-L.; Ding, S.-Y.; Zhang, Z.-C.; Wang, Z.-P.; Wang, W. Constructing Robust Covalent Organic Frameworks via Multicomponent Reactions. *J. Am. Chem. Soc.* **2019**, *141*, 18004−18008.

(11) Li, X.-T.; Zou, J.; Wang, T.-H.; Ma, H.-C.; Chen, G.-J.; Dong, Y.-B. Construction of Covalent Organic Frameworks via Three-Component One-Pot Strecker and Povarov Reactions. *J. Am. Chem. Soc.* **2020**, *142*, 6521−6526.

(12) Segura, J. L.; Royuela, S.; Mar Ramos, M. Post-Synthetic Modification of Covalent Organic Frameworks. *Chem. Soc. Rev.* **2019**, *48*, 3903−3945.

(13) Soleymani, M.; Chegeni, M. The Chemistry and Applications of the Quinoxaline Compounds. *Curr. Org. Chem.* **2019**, *23*, 1789−1827.

(14) Naibi Lakshminarayana, A.; Ong, A.; Chi, C. Modification of Acenes for N-Channel OFET Materials. *J. Mater. Chem. C* **2018**, *6*, 3551−3563.

(15) Gedefaw, D.; Prosa, M.; Bolognesi, M.; Seri, M.; Andersson, M. R. Recent Development of Quinoxaline Based Polymers/Small Molecules for Organic Photovoltaics. *Adv. Energy Mater.* **2017**, *7*, No. 1700575.

(16) Chua, M. H.; Zhu, Q.; Tang, T.; Shah, K. W.; Xu, J. Diversity of Electron Acceptor Groups in Donor−Acceptor Type Electrochromic Conjugated Polymers. *Solar Energy Mater. Solar Cells* **2019**, *197*, 32−75.

(17) Podsiadły, R. Photoreaction and Photopolymerization Studies on Fluoflavin Dye−Pyridinium Salt Systems. *J. Photochem. Photobiol. A: Chem.* **2008**, *198*, 60−68.

(18) Guirado, A.; López-Sánchez, J. I.; Cerezo, A.; Bautista, D.; Gálvez, J. A New and Efficient Synthetic Approach to Dichlorofluoflavines. Study of the Stability of Isomeric Fluoflavines by HF and B3LYP Procedures. *Tetrahedron* **2009**, *65*, 2254−2259.

(19) Zhang, B.; Wei, M.; Mao, H.; Pei, X.; Alshmimri, S. A.; Reimer, J. A.; Yaghi, O. M. Crystalline Dioxin-Linked Covalent Organic Frameworks from Irreversible Reactions. *J. Am. Chem. Soc.* **2018**, *140*, 12715−12719.

(20) Guan, X.; Li, H.; Ma, Y.; Xue, M.; Fang, Q.; Yan, Y.; Valtchev, V.; Qiu, S. Chemically Stable Polyarylether-Based Covalent Organic Frameworks. *Nat. Chem.* **2019**, *11*, 587−594.

(21) Chen, T.; Li, W.-Q.; Hu, W.-B.; Hu, W.-J.; Liu, Y. A.; Yang, H.; Wen, K. Direct Synthesis of Covalent Triazine-Based Frameworks (CTFs) through Aromatic Nucleophilic Substitution Reactions. *RSC Adv.* **2019**, *9*, 18008−18012.

(22) Kanakarajan, K.; Czarnik, A. W. Synthesis and Some Reactions of Hexaazatriphenylenehexanitrile, a Hydrogen-Free Polyfunctional Heterocycle with D3h Symmetry. *J. Org. Chem.* **1986**, *51*, 5241−5243.

(23) Walczak, R.; Kurpil, B.; Savateev, A.; Heil, T.; Schmidt, J.; Qin, Q.; Antonietti, M.; Oschatz, M. Template- and Metal-Free Synthesis of Nitrogen-Rich Nanoporous "Noble" Carbon Materials by Direct Pyrolysis of a Preorganized Hexaazatriphenylene Precursor. *Angew. Chem. Int. Ed.* **2018**, *57*, 10765−10770.

(24) Fenton, J. L.; Burke, D. W.; Qian, D.; Olvera de la Cruz, M.; Dichtel, W. R. Polycrystalline Covalent Organic Framework Films Act as Adsorbents, Not Membranes. *J. Am. Chem. Soc.* **2021**, *143*, 1466−1473.

https://doi.org/10.1021/acsami.1c08854
ACS Appl. Mater. Interfaces 2021, 13, 37494−37499